

Physiologically Based Pharmacokinetic (PBPK) Model for Biodistribution of Radiolabeled Peptides in Patients with Neuroendocrine Tumours

Radovan Gospavic^{1,2}, Peter Knoll³, Siroos Mirzaei³, Viktor Popov^{1*}

¹ Ascend Technologies Ltd, Eastleigh, UK

² Faculty of Civil Engineering, University of Belgrade, Belgrade, Serbia

³ Institute of Nuclear Medicine with PET-Center, Wilhelminenspital, Vienna, Austria

ARTICLE INFO

Article type:

Original article

Article history:

Received: 21 Jan 2016

Revised: 30 Mar 2016

Accepted: 10 Apr 2016

Keywords:

Lu-177 DOTATATE

PBPK model

Radiolabeled peptides

Whole body scintigraphy

ABSTRACT

Objective(s): The objectives of this work was to assess the benefits of the application of Physiologically Based Pharmacokinetic (PBPK) models in patients with different neuroendocrine tumours (NET) who were treated with Lu-177 DOTATATE. The model utilises clinical data on biodistribution of radiolabeled peptides (RLPs) obtained by whole body scintigraphy (WBS) of the patients.

Methods: The blood flow restricted (perfusion rate limited) type of the PBPK model for biodistribution of radiolabeled peptides (RLPs) in individual human organs is based on the multi-compartment approach, which takes into account the main physiological processes in the organism: absorption, distribution, metabolism and excretion (ADME). The approach calibrates the PBPK model for each patient in order to increase the accuracy of the dose estimation. Datasets obtained using WBS in four patients have been used to obtain the unknown model parameters. The scintigraphic data were acquired using a double head gamma camera in patients with different neuroendocrine tumours who were treated with Lu-177 DOTATATE. The activity administered to each patient was 7400 MBq.

Results: Satisfactory agreement of the model predictions with the data obtained from the WBS for each patient has been achieved.

Conclusion: The study indicates that the PBPK model can be used for more accurate calculation of biodistribution and absorbed doses in patients. This approach is the first attempt of utilizing scintigraphic data in PBPK models, which was obtained during Lu-177 peptide therapy of patients with NET.

► Please cite this paper as:

Gospavic R, Knoll P, Mirzaei S, Popov V. Physiologically Based Pharmacokinetic (PBPK) Model for Biodistribution of Radiolabeled Peptides in Patients with Neuroendocrine Tumours. Asia Oceania J Nucl Med Biol. 2016; 4(2): 90-97. doi: 10.7508/aojnmb.2016.02.005

Introduction

For the development of new therapeutic agents and drugs Physiologically Based Pharmacokinetic (PBPK) models have been used as a tool for the estimation of the biodistribution and toxicity of different chemical compounds and macromolecules in the living organisms (1-4). The results obtained from such models have been used in the pharmaceutical industry to assess the

time course of the drugs in targeted tissues and for toxicity analysis and estimation in the case of the non-targeted tissues in living organisms (5,6). The PBPK models have also been used in environmental and risk assessment applications (7-9). The main area of interest and research in PBPK modelling is to determine and analyse the fate of drugs, macromolecules or other chemical

* Corresponding author: Viktor Popov, Ascend Technologies Ltd, Wessex House, Upper Market Street, Eastleigh, SO50 9FD, UK. Tel: +44 2381 783600; Email: viktor@ascendtechnologies.co.uk

© 2016 mums.ac.ir All rights reserved.

This is an Open Access article distributed under the terms of the Creative Commons Attribution License (<http://creativecommons.org/licenses/by/3.0>), which permits unrestricted use, distribution, and reproduction in any medium, provided the original work is properly cited.

compounds administrated externally into living organisms. The four basic physiological processes in the living organisms which determine fate of the drugs and chemicals administrated into organisms are: absorption, distribution, metabolism and excretion (ADME) (1,2).

PBPK models consist of compartments which represent organs, tissues, blood, and these compartments are connected by blood circulation. The pharmacokinetic in living organisms is very complex and depends on physical and chemical properties of drugs and macromolecules, blood flow, physical and chemical characteristics of tissues and organs, tissue composition, permeability of various tissue membranes (10). In many cases experimental data is only available for animals and interspecies scaling could be used to extrapolate PBPK model from animals to humans (11).

In the last two decades there has been an increase of radionuclide treatment of cancer. The regulations on patient safety require adherence to standards such as calculation of biodistribution and absorbed patient dose. Also, the toxicity to healthy organs cannot be neglected and has to be considered (12). For example, for patients treated with radionuclide labeled somatostatin analogs, the renal absorbed dose plays a major role in further patient specific optimized therapy dose estimation (13), which can be calculated from sequential scintigraphic images with gamma cameras. The recent guidelines describe the good practice of clinical dosimetry reporting and proper dosimetric assessment of nuclear medicine diagnostic and therapeutic agents (14,15).

An approach employing the PBPK can be used to determine the appropriate therapeutic dose in cancer patients (16). One aspect that reduces the accuracy of these estimates is the physiological variability in patients. Another aspect is that in cancer patients this variability may be even higher since organs may be affected to different levels depending on the type of cancer and in some cases as a side effect of the applied chemotherapy. Stabin et al. has argued that the combined uncertainties in any given radiopharmaceutical dose estimate are a factor of 2 or higher, mainly because of human variability which can be increased due to disease (17).

The clinical data on biodistribution of therapeutic drugs in human patients could be of practical importance for the development of the PBPK models to improve cancer therapy.

In this work a blood flow restricted PBPK approach has been implemented and tested in patients with different neuroendocrine tumours who were treated with Lu177- DOTATATE. The main assumption in the blood flow restricted type of PBPK model is that the

considered tissue or organ could be approximated as a well-stirred compartment (18,19). In some cases the PBPK models are used in combination with in vitro data prior to the in vivo experiments in order to predict the plasma and tissue pharmacokinetics of a drug (1). Most of the previous work on PBPK models have focused on determining the model parameters for certain species.

In the present approach calibration of the PBPK model is carried out for each patient. The calibration is carried out using clinical data on the biodistribution of RLPs obtained by whole body scintigraphy of the patients.

The model is expected to provide increased accuracy when selecting the radiation dose. One reason for this is that the model considers the whole injected dose and applies the mass conservation taking into account the distribution of the radiopharmaceutical in the body and its clearance, based on information about the human physiology. In this way the time-dependent activity can be obtained for different tissues, which can further be used to determine the average absorbed dose per tissue/organ. In this way one can appropriately select the radiation dose in order to balance the risks and the benefits.

Another potential application, which was not implemented in this work, would be to monitor the patient's condition through a comparison of the model predictions and the clinical data on the biodistribution of RLPs. Large disagreements of the model and the clinical data might indicate change in the patient's condition.

To solve the optimization problem and to obtain the unknown model parameters the trust region method has been utilized. To speed up the numerical procedure the Broyden-Fletcher-Goldfarb-Shanno (BFGS) method has been used (20-23).

Methods

In this study the scintigraphic data were used, which were acquired with a double head gamma camera (Symbia T6, Siemens, Erlangen, Germany) in patients with different neuroendocrine tumours who were treated with Lu177- DOTATATE (Lutathera®, AAA, France). The activity administered to each patient was 7400 MBq (24).

It has been reported that the kidney is the dose-limiting organ in the RLPs therapies. In order to reduce the uptake of RLPs in the kidneys, each patient received an intravenous injection of a fixed combination of amino acids arginine and lysine, as recommended previously by several studies (25-27). Planar whole body imaging was performed at 0.5, 4, 24, 48 h and/or 72 h post injection for

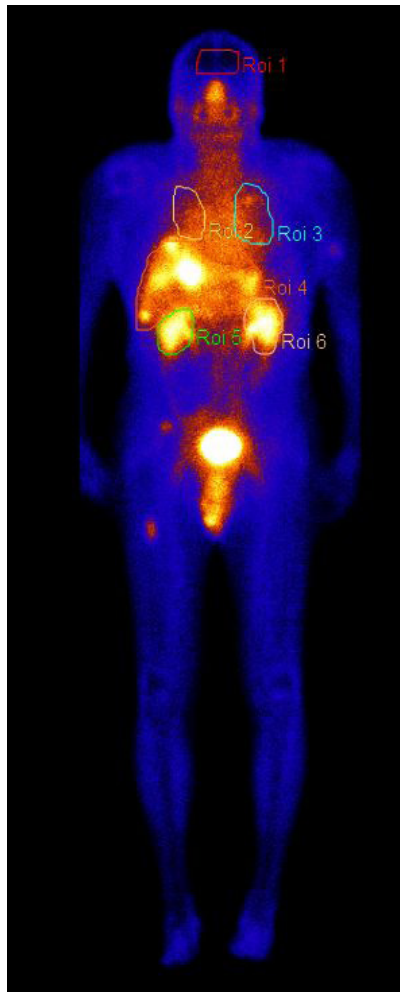


Figure 1. Whole body image showing radiotracer distribution in different regions of interests (ROI) over brain, lungs, kidneys and liver

all the patients. The first whole body image was performed with full bladder and was used for normalization. Figure 1 shows WBS image with regions of interest (ROI): brain, lungs, kidneys and liver.

**Mathematical Model
PBPK Modelling**

Radiation dose estimates for radiopharmace-

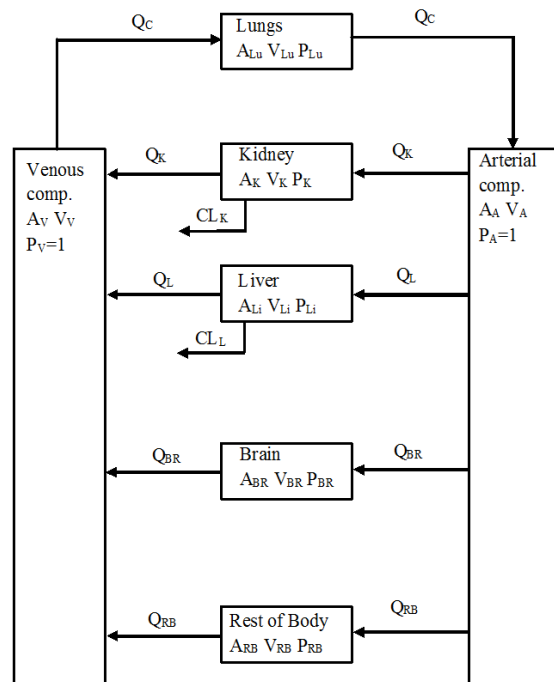


Figure 2. Schematic diagram for multi compartment PBPK model for biodistribution of Lu177- DOTATATE in human body

uticals are of importance in cancer therapy applications. Any improvement in the accuracy of the estimate would lead to a better balance between the risks and benefits of the therapy.

The average absorbed dose in target tissue is estimated as:

$$A_d = \frac{k\hat{A}\sum_i x_i E_i f_i}{M} \tag{1}$$

where A_d is mean absorbed dose (Gy) to a target tissue; \hat{A} is the time-activity integral within the target tissue (Bq s); x_i is the number of radiations with energy E_i per nuclear transition; E_i is the mean energy of the i -th radiation (MeV); f_i is the fraction for the i -th radiation absorbed in target tissue; M is the mass of the target tissue (kg); k is a constant ($\text{Gy kg Bq}^{-1} \text{s}^{-1} \text{MeV}^{-1}$).

The time-activity integral \hat{A} is calculated as an

Table 1. Nomenclature used for the PBPK model

Q_c [ml/min]	Total Cardiac output
Q_T [ml/min]	Blood flow for individual tissue/organ
V_T [ml]	Volume of the tissue/organ
A_T [Bq/ml]	activity in tissue/organ
P_T	Tissue to blood partition coefficients
CL_T [Bq/min]	Clearance or metabolic parameter

Lu: Lung, K: Kidney, L: Liver, RB: Rest of Body, A: Arterial compartment, V: Venous compartment, BR: brain

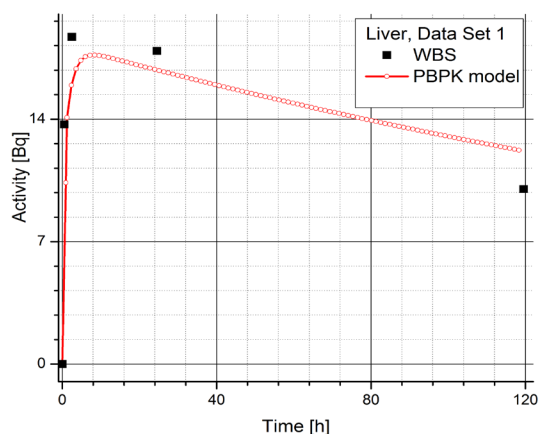


Figure 3. Comparison of time-activity curves in liver for patient 1, obtained by WBS and PBPK model

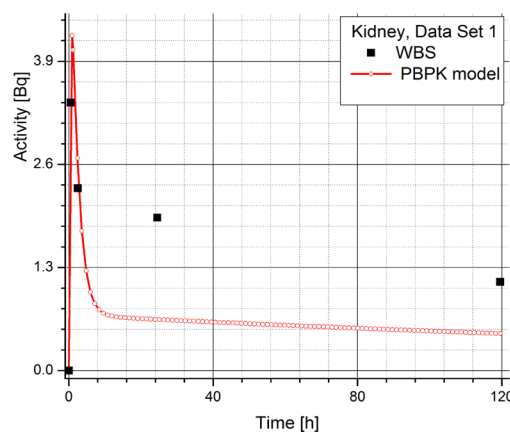


Figure 4. Comparison of time-activity curve in kidney for patient 1, obtained by WBS and PBPK model

integral of the time-dependent activity A [Bq]

$$\hat{A} = \int_0^{\infty} A(t)dt = A_0 \int_0^{\infty} \alpha(t)dt \quad (2)$$

where A_0 is the activity administered at time $t = 0$, and $\alpha(t)$ is the fraction of the administered activity present within the source region at time t . In this work the average absorbed dose is not calculated as the main focus is on PBPK model development for determining the time-dependent activity A . Once A is available, it is straightforward to calculate the time-activity integral and the average absorbed dose in a tissue.

The blood flow restricted type of the PBPK model with seven compartments was developed and was used for prediction of biodistribution and accumulation in different organs in the human body. The schematic diagram of the PBPK model with

different compartments is shown in Figure 2. The nomenclature used in the Figure 1 is summarised in Table 1.

To calibrate the model and find unknown model parameters the clinical results for four patients obtained by WBS have been used. The developed PBPK model includes the following organs: lungs, kidney, liver, brain, venous and arterial compartments and the rest of body. The results from the WBS include the whole body; however, results suggest that biodistribution occurs mainly in the liver and kidneys.

The main assumptions in the model are: (i) each tissue is modelled as homogenous, (ii) the concentration of radiopharmaceuticals in the venous blood is in equilibrium with the concentration in the tissue and the model parameters (blood flow, tissues volumes and tissue to blood partition coefficients) are considered to be constant over time.

Table 2. Clinical results obtained by WBS for four different patients (Datasets 1 - 4). All quantities related to activity in specific organs are expressed in counts/sec (Bq)

Dataset 1				Dataset 2			
Time [h]	Liver	Kidney	Brain	time [h]	Liver	Kidney	Brain
0	0	0	0	0	0	0	0
0.5	13.70	3.38	0	0.5	2.41	3.60	0.05
2.5	18.70	2.30	0	3.5	1.38	1.73	0.2
24.5	17.90	1.93	0	23.5	0.98	1.50	0.15
119.5	10.00	1.12	0	119.5	0.33	0.27	0.066
Dataset 3				Dataset 4			
Time [h]	Liver	Kidney	Brain	time [h]	Liver	Kidney	Brain
0	0	0	0	0	0	0	0
0.5	5.75	2.12	0.15	0.5	7.5	2.28	0
2.5	6.05	1.31	0.20	4.5	7.79	1.92	0
20.5	5.50	1.36	0.02	26.5	7.2	1.81	0
71.5	3.57	0.74	0.0	69.5	5.2	1.22	0

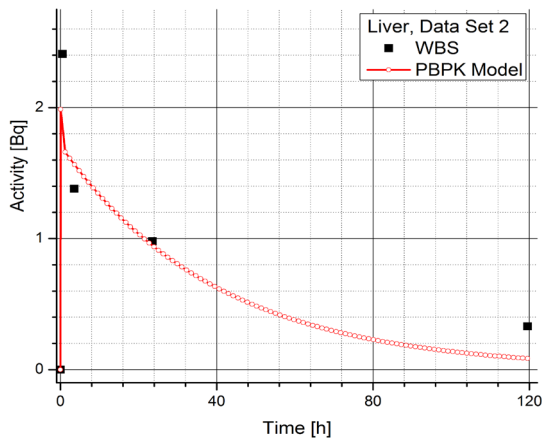


Figure 5. Comparison of time-activity curve in liver for patient 2, obtained by WBS and PBPK model

In the PBPK model, see Figure 2, due to mass conservation the following constraint related to blood flow must be satisfied:

$$Q_C = Q_{LU} = Q_K + Q_L + Q_{BR} + Q_{RB} \quad (3)$$

The balance equation for the case of flow perfusion-limited model for each non-clearing organ, which are the organs that do not remove/extract, except for the case of lungs and arterial and venous compartments, is given as (28 ,29):

$$V_T \frac{dA_T}{dt} = Q_T \cdot \left(A_A - \frac{A_T}{P_T} \right) \quad (4)$$

The balance equations for lungs, arterial and venous compartment are given in the following form (28 ,29):

$$V_{Lu} \frac{dA_{Lu}}{dt} = Q_c \cdot \left(A_V - \frac{A_{Lu}}{P_{Lu}} \right); \quad V_A \frac{dA_A}{dt} = Q_c \cdot \left(\frac{A_{Lu}}{P_{Lu}} - A_A \right);$$

$$V_V \frac{dA_V}{dt} = \sum_{T \neq Lu} Q_T \cdot \frac{A_T}{P_T} - Q_c \cdot \frac{A_{Lu}}{P_{Lu}} \quad (5)$$

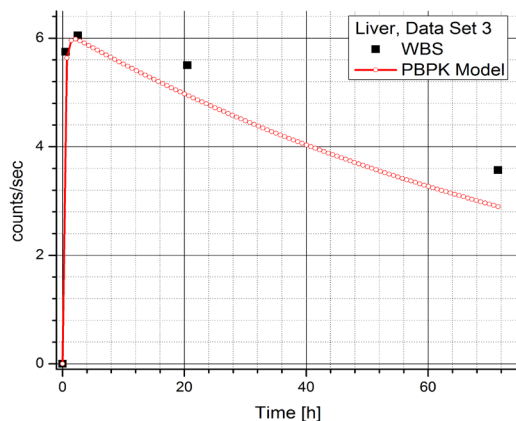


Figure 7. Comparison of time-activity curve in liver for patient 3, obtained by WBS and PBPK model

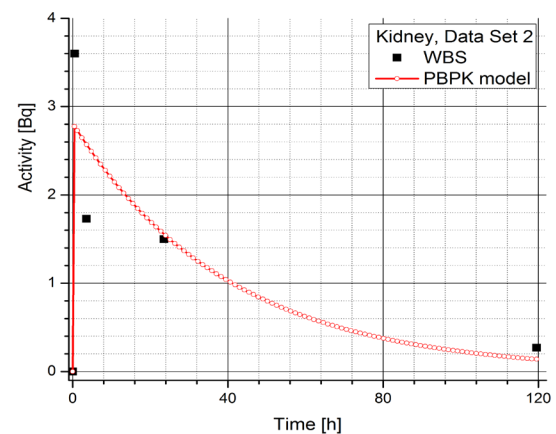


Figure 6. Comparison of time-activity curve in kidney for patient 2, obtained by WBS and PBPK model

For the case of organs with clearing or extraction, e.g. kidney, or metabolic processes, e.g. liver, the balance has been expressed in terms of intrinsic clearance CL by the following relation (28 ,29):

$$V_T \frac{dA_T}{dt} = Q_T \cdot A_A - \frac{(Q_T + CL_T)}{P_T} \cdot A_T \quad (6)$$

For the blood flow restricted type of models the unknown parameters, which depend on the type of drug, the macromolecule of compound, and the individual organ/tissue, include: partition coefficients P_T (which are responsible for absorption and distribution in the organs/tissues), for the case of tissue without clearance, and partition coefficients P_T and clearance CL [ml/min], for the case of tissue with clearance. The tissue/blood partition coefficient is defined as the ratio of concentration of radiopharmaceutical in tissue to that in the emergent venous blood of the tissue. The partition coefficients for chemicals/small molecules can be estimated from in vitro and/or in vivo methods (30).

It has been adopted that the average density of all organs/tissues is approximately 1 g/ml

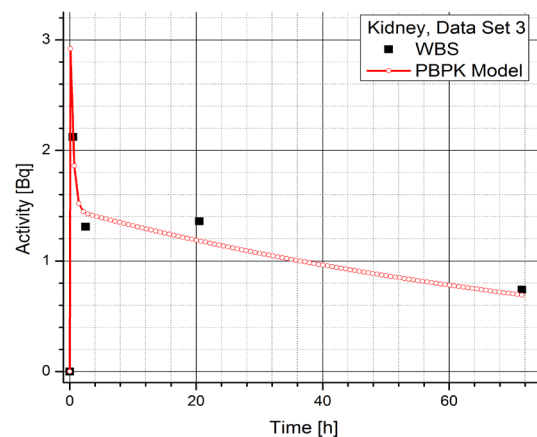


Figure 8. Comparison of time-activity curve in kidney for patient 3, obtained by WBS and PBPK model

(1.056 g/ml). Cardiac output per body weight for humans is estimated to 15 [L/h·kg^{0.74}] (7, 9, 31).

The mass of organs and fraction of blood flow for different organs in humans used to optimize the PBPK model are shown in Table 3e(7,9,31). Because the Blood Brain Barrier (BBB) restricts the transport of the large molecules from CBV to interstitial and cellular space of the Central Nervous System (CNS) it has been assumed that biodistribution of RLPs in the brain occurs only in CBV (32,33). According to this assumption, the available volume/mass of the brain in the PBPK model for biodistribution is 3.8% of total brain volume/mass, and is negligible for further measurements.

Estimation of the model parameters

The clinical data obtained by WBS was used to obtain the unknown model parameters. This procedure represents the calibration of the model and is equivalent to an optimization problem of finding the model parameters for which the difference between results obtained by model and clinical data are minimal. The difference between model results and clinical data is defined by the objective function. In this work the trust region method has been utilized to minimize the objective function and to obtain the optimal parameters in the PBPK model (34,35).

In the k-th iteration the objective function is approximated by the first two terms in the Taylor-series expansion inside the trust interval around the point P_k according to the following equations (36,37):

$$M_k(\Delta P) = F(P_k) + G_k^T \cdot \Delta P + \frac{1}{2} \Delta P^T \cdot H_k \cdot \Delta P; \quad \Delta P = P - P_k;$$

$$G_k = \left[\frac{\partial F}{\partial P_1}, \dots, \frac{\partial F}{\partial P_M} \right]_{P=P_k}; \quad H_k = \left[\frac{\partial^2 F}{\partial x_i \partial x_j} \right]_{P=P_k}; \quad (7)$$

$$F(P_k + \Delta P) \approx M_k(\Delta P); \quad \|\Delta P\| \leq D; \quad \|\Delta P\| = \sqrt{\sum_{i=1}^M \Delta P_i^2},$$

Table 3. Mass of organs and fraction of blood flow in humans used in the PBPK model

Organ/tissue	Weight [g]	Fraction of blood flow [%]
Lungs	1000	100
Kidney	299	22
Liver	1910	17.5
Brain	1420 ^a	11.4
Venous blood	2350 (2.35 L)	100
Rest of body	64371	49.1
Arterial blood	2350 (2.35 L)	100

a- Intravascular compartment (vascular space) or cerebral blood volume (CBV) =3.8%, Extracellular space (ECS) = interstitial space + CBV = 15 - 20%, cellular space = 80 - 95%

where F is the objective function, M_k is quadratic model function for F in the k-th iteration, G_k and H_k are gradient and Hessian matrix of the objective function at point P_k, respectively, D is radius of the trust region, ||ΔP|| is the Euclidian norm of ΔP, G_k is 1×N vector and H_k is N×N symmetric matrix.

The model function is minimized inside the trust region (sub problem) under constraints that all model parameters are positive and the k+ 1 point P_{k+1} is obtained according to the following relations:

$$\min_{\Delta P} (M_k(\Delta P)), \quad \|\Delta P\| \leq D_k, \quad P_i + \Delta P_i > 0$$

$$\rightarrow \Delta P_k; \quad P_{k+1} = P_k + \Delta P_k \quad (8)$$

To speed up the numerical procedure, the trust region method has been modified and the Hessian matrix H_k is approximated using Broyden-Fletcher-Goldfarb-Shanno (BFGS) Method (20-23).

In each iteration the Hessian matrix is updated using the data from the previous step according to the following relation:

$$H_{k+1} = H_k + \frac{\gamma_k \cdot \gamma_k^T}{\gamma_k^T \cdot \delta_k} - \frac{H_k \cdot \delta_k \cdot \delta_k^T \cdot H_k}{\delta_k^T \cdot H_k \cdot \delta_k};$$

$$\delta_k = \Delta P_{k+1} - \Delta P_k; \quad \gamma_k = G_{k+1} - G_k \quad (9)$$

Results

Table 2 contains the clinical data showing radiopharmaceuticals' activities in organs (dataset 1-4) which are expressed in counts per second (Bq). The data has been obtained using WBS of patients with NET treated with Lu177- DOTATATE and it suggests a large inter-individual variability in the patients, which prevents using same model parameters for all the patients. Figures 3 and 4 show the change in time of activity in liver and kidney, respectively, obtained for the dataset 1 by WBS and by the PBPK model. The activity of RLP is expressed in Becquerel [Bq]. Figures 5 - 8, show the similar data to Figures 3 and 4. It is evident that in each case a good agreement is achieved between the model and the WBS data, except for the case of activity in kidneys for dataset 1 where delayed kidney clearance rate is observed for the model results compared to the WBS recordings. While this discrepancy seems prominent, a comparative magnitude of discrepancy is observed in Figure 3 for the activity in liver for dataset 1, except that the activity in liver is by one order of magnitude higher compared to kidneys, so the discrepancy seems smaller.

Discussion

The blood flow restricted (perfusion rate

limited) type of PBPK model for biodistribution and accumulation in individual organs has been developed for Lu177- DOTATATE using clinical data obtained by whole body scintigraphy (WBS) in four different patients. This is the first attempt of utilizing scintigraphic data from therapy of patients with NET with Lu177- peptides in PBPK models. However, the limitation of the study is the low number of the patients available and not applying SPECT results for increased precision in measurements of the activity distributions in the organs.

According to the available data, a PBPK model with seven compartments has been adopted. The model takes into account the four main physiological processes in the organism: Absorption, Distribution, Metabolism and Extraction (ADME). The clearing tissue has been modelled using intrinsic clearance parameter.

The clinical results obtained by WBS for four different patients, see Table 2, show that there is significant difference in the RLPs distribution in different organs in time between different patients. The current results suggest that an approach would be feasible where a PBPK model is calibrated for each patient. This would lead to more accurate extrapolation of the time-activity data when the data on uptake and clearance is not collected for long enough period. The approach also allows for straightforward integration of the time-dependent activity providing increased accuracy and convenience when calculating the absorbed dose in certain tissue/organ. This approach eliminates the problems with inter-patient variability of RLPs distribution due to physiological differences or due to influence of disease and/or therapy. The calibration was carried out using clinical data on biodistribution of RLPs obtained by WBS of the patients. The numerical procedure for calibration of the model parameters has employed the trust-region method. To reduce the required CPU time and to speed up the simulation, the Hessian matrix has been approximated using Broyden-Fletcher-Goldfarb-Shanno (BFGS) method.

From the WBS data it could be observed that for some organs (dataset 1: kidneys; dataset 2: kidneys, liver and brain; dataset 3: kidneys) there is a rapid increase in concentrations of RLPs immediately after administration, which the model was able to reproduce.

The agreement of the model predictions with the data obtained from the WBS is satisfactory, indicating that the PBPK model presented in this study can be used for more accurate calculation of biodistribution of RLPs and more accurate

estimation of the absorbed dose in specific tissues/organs in the RLP therapies.

Conclusion

The study indicates that the PBPK model can be used for more accurate calculation of biodistribution and absorbed doses in patients. This approach is the first attempt of utilizing scintigraphic data in PBPK models, which was obtained during Lu177- peptide therapy of patients with NET.

Acknowledgments

The present study was supported by the SaveMe project, Project ID: 263307, as part of the Seventh Framework Programme, Theme NMP-2010-4.0-1- Development of nanotechnology-based systems for detection, diagnosis and therapy for cancers.

References

1. Theil FP, Guentert TW, Haddad S, Poulin P. Utility of physiologically based pharmacokinetic models to drug development and rational drug discovery candidate selection. *Toxicol Lett.* 2003;138(1-2):29-49.
2. Lee HA, Leavens TL, Mason SE, Monteiro-Riviere NA, Riviere JE. Comparison of quantum dot biodistribution with a blood-flow-limited physiologically based pharmacokinetic model. *Nano Lett.* 2009;9(2):794-9.
3. Baxter LT, Zhu H, Mackensen DG, Butler WF, Jain RK. Biodistribution of monoclonal antibodies: scale-up from mouse to human using a physiologically based pharmacokinetic model. *Cancer Res.* 1995;55(20):4611-22.
4. Baxter LT, Zhu H, Mackensen DG, Jain RK. Physiologically based pharmacokinetic model for specific and nonspecific monoclonal antibodies and fragments in normal tissues and human tumor xenografts in nude mice. *Cancer Res.* 1994;54(6):1517-28.
5. Adams JC, Dills RL, Morgan MS, Kalman DA, Pierce CH. A physiologically based toxicokinetic model of inhalation exposure to xylenes in Caucasian men. *Regul Toxicol Pharmacol.* 2005;43(2):203-14.
6. Van Asperen J, Rijcken WR, Lammers JH. Application of physiologically based toxicokinetic modelling to study the impact of the exposure scenario on the toxicokinetics and the behavioural effects of toluene in rats. *Toxicol Lett.* 2003;138(1-2):51-62.
7. Sweeney LM, Gut CP Jr, Gargas ML, Reddy G, Williams LR, Johnson MS. Assessing the non-cancer risk for RDX (hexahydro-1,3,5-trinitro-1,3,5-triazine) using physiologically based pharmacokinetic (PBTK) modelling. *Regul Toxicol Pharmacol.* 2012;62(1):107-14.
8. Krishnan K, Peyret T. Physiologically based

- toxicokinetic (PBTK) modeling in ecotoxicology. In *Ecotoxicology modeling/modelling*. New York: Springer; 2009. (ppP. 145-175). Springer US
9. Clewell RA, Clewell HJ 3rd. Development and specification of physiologically based pharmacokinetic models for use in risk assessment. *Regul Toxicol Pharmacol*. 2008;50(1):129-43.
 10. Nestorov I. Whole-Body Physiologically Based Pharmacokinetic Models. *Expert Opin Drug Metab Toxicol*. 2007;3(2):235-49.
 11. Ings RM. Interspecies scaling and comparisons in drug development and toxicokinetics. *Xenobiotica*. 1990;20(11):1201-31.
 12. Bodei L, Kidd M, Paganelli G, Grana CM, Drozdov I, Cremonesi M, et al. Long-term tolerability of PRRT in 807 patients with neuroendocrine tumours: the value and limitations of clinical factors. *Eur J Nucl Med Mol Imaging*. 2015;42(1):5-19.
 13. Barone R, Borson-Chazot F, Valkema R, Walrand S, Chauvin F, Gogou L, et al. Patient-specific dosimetry in predicting renal toxicity with (90)Y-DOTATOC: relevance of kidney volume and dose rate in finding a dose-effect relationship. *J Nucl Med*. 2005;46(Suppl 1):99S-106S.
 14. Lassmann M, Chiesa C, Flux G, Bardiès M, EANM Dosimetry Committee. EANM Dosimetry Committee guidance document: good practice of clinical dosimetry reporting. *Eur J Nucl Med Mol Imaging*. 2011;38(1):192-200.
 15. 1990 Recommendations of the International Commission on Radiological Protection.. *Ann ICRP*. 1991;21(1-3):1-201.
 16. Yamashita F, Hashida M. Pharmacokinetic considerations for targeted drug delivery. *Adv Drug Deliv Rev*. 2013;65(1):139-47.
 17. Stabin MG. Uncertainties in internal dose calculations for radiopharmaceuticals. *J Nucl Med*. 2008;49(5):853-60.
 18. Gerlowski LE, Jain RK. Physiologically based pharmacokinetic modelling: principles and applications. *J Pharm Sci*. 1983;72(10):1103-27.
 19. Davies B, Morris T. Physiological Parameters in laboratory animals and humans. *Pharm Res*. 1993;10(7):1093-5.
 20. Broyden CG. Quasi-Newton methods and their application to function minimization. *Maths Comput*. 1967;21(99):368-81.
 21. Fletcher R. A new approach to variable metric algorithms. *Computer J*. 1970;13(3):317-22.
 22. Goldfarb D. A family of variable-metric methods derived by variational means. *Maths Comput*. 1970;24(109):23-26.
 23. Shanno DF. Conditioning of quasi-Newton methods for function minimization. *Maths Comput*. 1970;24(111):647-56.
 24. Mirzaei S, Bastati B, Lipp RW, Knoll P, Zojer N, Ludwig H. Additional lesions detected in therapeutic scans with ¹⁷⁷Lu-DOTATATE reflect higher affinity of ¹⁷⁷Lu-DOTATATE for somatostatin receptors. *Oncology*. 2011;80(5-6):326-9.
 25. Rolleman EJ, Valkema R, de Jong M, Kooij PP, Krenning EP. Safe and effective inhibition of renal uptake of radiolabelled octreotide by a combination of lysine and arginine. *Eur J Nucl Med Mol Imaging*. 2003;30(1):9-15.
 26. Vegt E, de Jong M, Wetzels JF, Masereeuw R, Melis M, Oyen WJ, et al. Renal toxicity of radiolabeled peptides and antibody fragments: mechanisms, impact on radionuclide therapy, and strategies for prevention. *J Nucl Med*. 2010;51(7):1049-58.
 27. Kwekkeboom DJ, de Herder WW, Kam BL, van Eijck CH, van Essen M, Kooij PP, et al. Treatment with the radiolabeled somatostatin analog [¹⁷⁷Lu-DOTA0,Tyr3] octreotate: toxicity, efficacy, and survival. *J Clin Oncol*. 2008;26(13):2124-30.
 28. Reddy M, Yang RS, Andersen ME, Clewell III HJ. Physiologically based pharmacokinetic modeling: science and application. Hoboken, New Jersey: John Wiley & Sons; 2005.
 29. Ball R, Schwartz SL. CMATRIX: software for physiologically based pharmacokinetic modeling using a symbolic matrix representation system. *Comput Biol Med*. 1994;24(4):269-76.
 30. Lin JH, Sugiyama Y, Awazu S, Hanano M. In vitro and in vivo evaluation of the tissue-to-blood partition coefficient for physiological pharmacokinetic models. *J Pharmacokinet Biopharm*. 1982; 10(6): 637-47.
 31. Hissink AM, Wormhoudt LW, Sherratt PJ, Hayes JD, Commandeur JN, Vermeulen NP, et al. A physiologically-based pharmacokinetic (PB-PK) model for ethylene dibromide: relevance of extrahepatic metabolism. *Food Chem Toxicol*. 2000;38(8):707-16.
 32. Pardridge WM. Blood-brain barrier biology and methodology. *J Neurovirol*. 1999;5(6):556-69.
 33. Banks WA. Physiology and pathology of the blood-brain barrier: implications for microbial pathogenesis, drug delivery and neurodegenerative disorders. *J Neurovirol*. 1999;5(6):538-55.
 34. Lueshen E, Hall C, Mošat A, Linninger A. Physiologically-Based Pharmacokinetic Modeling: Parameter Estimation for Cyclosporin A. In: Pistikopoulos EN, Georgiadis MC, Kokossis AC, editors. 21st European Symposium on Computer Aided Process Engineering. 1st ed. Philadelphia: Elsevier; 2011. P. 1543.
 35. Toint PL. Toint PL. Global convergence of trust-region methods for nonconvex minimization in hilbert space. *IMA J Numerical Anal*. 1988;8(2):231-52.
 36. Nocedal J, Wright S. Numerical optimization. 2nd ed. New York: Springer Science & Business Media; 2006.
 37. Conn AR, Gould NI, Toint PL. Trust-region methods, society for industrial and applied mathematics. SIAM, Philadelphia. 2000;1(7):12.